

Synthesis, Structural And Luminescence Properties Of Tm^{3+} Ions Activated Oxyapatite Structured $\text{Sr}_2\text{Gd}_8(\text{SiO}_4)_6\text{O}_2$ Phosphors

Dr.G.Manikya Rao

Head of the Department of Physics,

C.R College, Chilakaluripet.

Abstract : The $\text{Sr}_2\text{Gd}_8(\text{SiO}_4)_6\text{O}_2 : \text{Tm}^{3+}$ Phosphors were successfully prepared using a citrate sol-gel method. The X-Ray diffraction pattern of $\text{Sr}_2\text{Gd}_8(\text{SiO}_4)_6\text{O}_2 : \text{Tm}^{3+}$ phosphor confirmed the Hexagonal oxyapatite crystal structure. The field emission scanning electron microscopy image exhibited a typical rod-like morphology. The $\text{Sr}_2\text{Gd}_8(\text{SiO}_4)_6\text{O}_2 : \text{Tm}^{3+}$ phosphors displayed an attractive photoluminescence properties. The PL spectra of SGSO: Tm^{3+} phosphors showed the intense blue emission at 454 nm with the corresponding electronic $^1\text{D}_2 \rightarrow ^3\text{F}_4$ transition. The CIE chromaticity coordinates of the PL spectra specifies that SGSO: Tm^{3+} phosphor is expected to be a promising material for potential applications in the development of efficient WLEDs and FED systems.

1. INTRODUCTION

We are concentrated on the investigation of trivalent thulium (Tm^{3+}) ions activated $\text{Sr}_2\text{Gd}_8(\text{SiO}_4)_6\text{O}_2$ phosphors synthesized by citrate sol-gel method. The aim of this work was to explore an efficient blue phosphor for the development of field emission displays (FEDs). Because, in recent years, FEDs have been attained an increasing attention as the most promising next generation flat panel displays due to their possible advantages including thin panel thickness, light weight, distortion-free image, wide viewing angle, self-emission, quick response time, low power consumption and high brightness/contrast ratio.¹⁻⁶ The thulium (Tm^{3+}) ions exhibit very interesting luminescence properties. The energy level of Tm^{3+} ion provides the possibility of a strong blue emission at 454 nm and a weak blue emission at 474 nm, which are assigned to the $^1\text{D}_2 \rightarrow ^3\text{F}_4$ (intense blue) and $^1\text{G}_4 \rightarrow ^3\text{H}_6$ (weak blue) electronic transitions respectively.⁷ The electronic transition $^1\text{D}_2 \rightarrow ^3\text{F}_4$ is known as hypersensitive and its intensity strongly depends on the host lattice, however, the transition $^4\text{F}_{9/2} \rightarrow ^6\text{H}_{15/2}$ is less sensitive. Because of very strong blue luminescence, Tm^{3+} ions are trustworthy as a suitable blue source and generate the possibility for the fabrication of white light emission to be used for FEDs. These interesting properties of Tm^{3+} ions encouraged us to investigate the luminescence properties of $\text{Sr}_2\text{Gd}_8(\text{SiO}_4)_6\text{O}_2 : \text{Tm}^{3+}$ phosphors.

The sulfide-based blue phosphors, such as, ZnS:Ag, ZnS:Cu,Al, $\text{SrGa}_2\text{S}_4:\text{Ce}^{3+}$, etc., are difficult to use in FEDs for long-term use because of their self-drawbacks (volatility, corrosive nature). Moreover, blue emitting oxides, such as, $\text{Y}_2\text{SiO}_5:\text{Ce}^{3+}$, Sr_2CeO_4 and $\text{YNbO}_4:\text{Bi}^{3+}$ generally

have lower efficiencies (due to their insulative properties) and lower color purity, which restrict their usage in FEDs. Thulium doped phosphors,⁸⁻¹³ such as, $\text{SrHfO}_3:\text{Tm}^{3+}$, $\text{Ba}_2\text{B}_5\text{O}_9\text{Cl}:\text{Tm}^{3+}$, $\text{Y}_3\text{GaO}_6:\text{Tm}^{3+}$, $\text{LaAlGe}_2\text{O}_7:\text{Tm}^{3+}$, $\text{LaGaO}_3:\text{Tm}^{3+}$, etc., are considered as most promising blue components with better color-rendering properties, appropriate lifetimes, and potential applications in cathode ray tube screens, plasma display panels, field emission displays and electroluminescent devices. But, the costly raw materials like HfO_2 , Ga_2O_3 , GeO_2 , etc., and high manufacturing costs greatly limit the usage of these phosphors in a large-scale synthesis. These entire drawbacks motivated us to investigate the suitable blue phosphor with good chromaticity and high efficiency for lighting and display applications.

In the literature, to the best of our knowledge, no reports have been found so far on the study of structural, morphological and luminescent properties of SGSO: Tm^{3+} phosphors. Therefore, in the present investigation, we have studied the structural, morphological and detailed luminescence properties of SGSO: Tm^{3+} phosphors prepared by the citrate sol-gel method.

2. EXPERIMENTAL DETAILS

2.1 Synthesis Method

Different concentrations of SGSO: Tm^{3+} phosphors were prepared with the composition $\text{Sr}_2(\text{Gd}_{1-x}\text{Tm}_x)_8\text{Si}_6\text{O}_{26}$ ($x = 0.5 - 5$ mol%) using a citrate sol-gel technique.

2.2 Characterizations

The structural properties of SGSO: Tm^{3+} phosphor powders were studied using X-ray diffraction (XRD) patterns (recorded on Mac Science M18XHF-SRA X-ray powder diffractometer). The

morphological properties were examined using high-resolution FE-SEM (HR FE-SEM) micrographs (recorded on HR FE-SEM: CARL ZEISS, MERLIN). The luminescence properties were studied using photoluminescence (PL) spectra (recorded on Scinco fs-2 fluorescence spectrometer).

3. RESULTS AND DISCUSSION

3.1. X-Ray Diffraction (XRD)

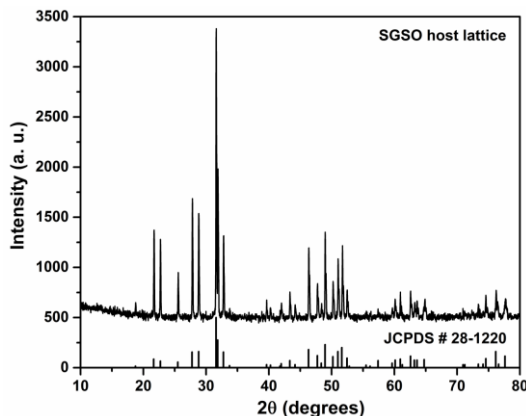


Fig.1(a). XRD pattern of SGSO host lattice.

Furthermore, no obvious shifting of peaks or any impurity phase in the XRD pattern due to Tm^{3+} ions can be identified at the current doping level, signifying that the doped ions are perfectly dissolved into the Gd^{3+} ion sites of SGSO host lattice. It is prominent that the pure phase of a phosphor is auspicious for better luminescent properties. The crystallite sizes were calculated using the Scherrer formula,^{14,15}

$$D_{hkl} = \frac{k\lambda}{\beta \cos\theta}$$

where D is the crystallite size, k (0.9) is the shape factor, λ is the X-ray wavelength used (1.5406 Å), β is the full width at half maximum and θ is the diffraction angle of an observed peak, respectively. The average crystallite sizes for pure SGSO and SGSO:2Tm³⁺ phosphors were found to be 70.8 nm and 71.7 nm respectively. The lattice parameters (a

In order to examine the phase formation and purity of Tm^{3+} ions doped SGSO host lattice, the XRD analysis was carried out. The XRD patterns of the pure SGSO host lattice and 2 mol% Tm^{3+} ions activated SGSO (i.e., SGSO:2Tm³⁺) phosphors were shown in the Figs, 1(a) and 1(b). It can be seen that all the diffraction peaks were in good agreement with the standard JCPDS card [PDF (28-1220)] and confirmed the hexagonal crystal form of oxyapatite structure with the space group of $\text{P6}_3/\text{m}$.

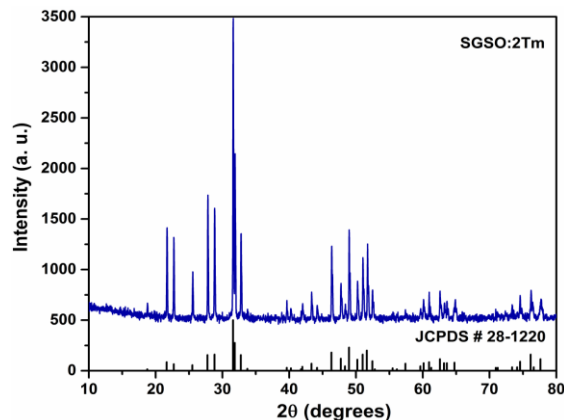


Fig.1(b). XRD pattern of SGSO:2Tm³⁺ phosphor.

and c) were also calculated for these phosphors using the formula for hexagonal structures,

$$\frac{1}{d^2} = \frac{4}{3} \left[\frac{h^2 + hk + k^2}{a^2} \right] + \frac{l^2}{c^2},$$

where d is the d-spacing and h , k , l are the Miller indices. The calculated values were $a = 9.418$ Å and $c = 6.941$ Å for SGSO host lattice and $a = 9.443$ Å and $c = 6.964$ Å for SGSO:2Tm³⁺ phosphors. The calculated lattice parameters were well matched with the values reported in the standard JCPDS card [PDF (28-1220)] ($a = 9.463$ Å and $c = 6.971$ Å). The good agreement in lattice parameter (a and c) values provides an evidence for the perfect incorporation of Tm^{3+} ions in the SGSO host lattice.

3.2. Scanning Electron Microscopy (SEM)

The morphological image of the SGSO:2Tm³⁺ phosphor, annealed at 1450 °C for 12 h, was shown in Fig.2.

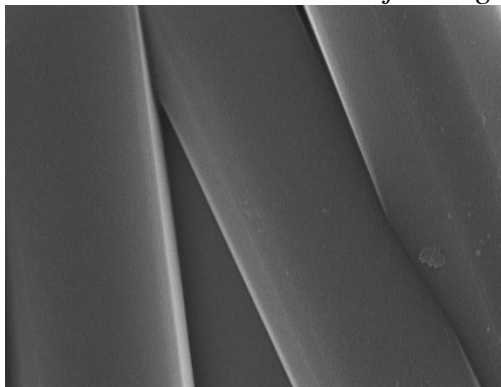


Fig.2. HR FE-SEM image of SGSO:2Tm³⁺ phosphor.

The particles acquired a sub-micron (100 nm) sized rod-like morphology with less aggregation and the typical rod-like morphology obtained at relative higher synthesis temperature is most favorable for phosphor powders to exhibit better emission properties.¹⁶ From the Fig.2, it is clear that the Tm³⁺

3.3. Photoluminescence (PL)

3.3.1. Photoluminescence excitation (PLE)

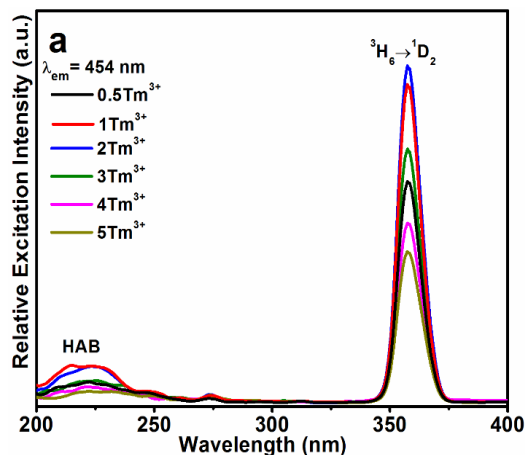
Fig.3 shows the PLE spectra of the SGSO:Tm³⁺ phosphors by monitoring the emission wavelength at 454 nm. The PLE spectra consisted of a weak broad band excitation below 250 nm in the higher energy regions called as host absorption band Fig.3. PLE spectra of the SGSO:Tm³⁺ phosphors as a function of Tm³⁺ ion concentration.

3.3.2 Photoluminescence emission (PL)

Fig.4 shows the PL spectra of the SGSO:Tm³⁺ phosphors as a function of Tm³⁺ ion concentration

ions are uniformly distributed into the Gd³⁺ ion sites in the SGSO host lattice. Therefore, the rod-like morphology and the uniform distribution of Tm³⁺ ions into the Gd³⁺ ion sites in the SGSO host lattice provide a good indication to attain efficient luminescent properties from SGSO:Tm³⁺ phosphors. (HAB). Also, an intense characteristic excitation peak at 357 nm in the lower energy regions due to the 4f¹² intra-configurational ³H₆→¹D₂ transition of Tm³⁺ ions was observed. From the PLE spectra, clearly, the Gd³⁺ ions did not exhibit prominent excitation peaks in the wavelength range of 250-320 nm due to the weak interactions between the Gd³⁺ and Tm³⁺ ions.

→ ³F₂ and ¹G₄ → ³F₄ transitions, respectively.¹⁷ The blue emission transition of ¹G₄ → ³H₆ at 474 nm



with an excitation wavelength of 357 nm. The PL spectra of SGSO:Tm³⁺ phosphors showed the intense blue emission at 454 nm with the corresponding electronic ¹D₂ → ³F₄ transition. A weak blue emission at 474 nm with the electronic transition of ¹G₄ → ³H₆ at the shoulder of the ¹D₂ → ³F₄ emission and also very weak green and red emissions were observed in the 507-522 and 642-676 nm wavelength regions with a band maxima at 516 and 665 nm related to ¹I₆

occurred due to the multiphonon non-radiative relaxation process from ¹D₂ level. The ¹I₆ → ³F₂ transition in the green region was indicated based on the earlier reports.⁷ The obtained results from the SGSO:Tm³⁺ phosphors are very similar to the CaGd₂(SiO₄)₄O₂:Tm³⁺ (CGSO:Tm³⁺) oxyapatite phosphors. As analogy to CGSO:Tm³⁺ phosphors,⁷ the SGSO:Tm³⁺ phosphors exhibit the strong blue emission, and all other emission bands acquired weak

or negligible intensities due to their similar crystal structure with CGSO.⁷ The Tm^{3+} ions doped SGSO phosphor samples were prepared as the concentration of Tm^{3+} ions started from 0.5 to 5 mol%. No change in the spectral shapes of the SGSO: Tm^{3+} phosphors as a function of Tm^{3+} ion concentration was observed. However, the blue emission intensities were increased with the increasing the Tm^{3+} ion concentration upto 2 mol% and then the intensities

were decreased due to the concentration quenching. Thus, 2 mol% is the optimum concentration of Tm^{3+} ions in the SGSO host lattice.

The concentration quenching might be the rise of non-radiative channels with concentration increment, prompting the interaction with the quenching centers in the energy transfer/cross-relaxation process of the adjacent Tm^{3+} ions.

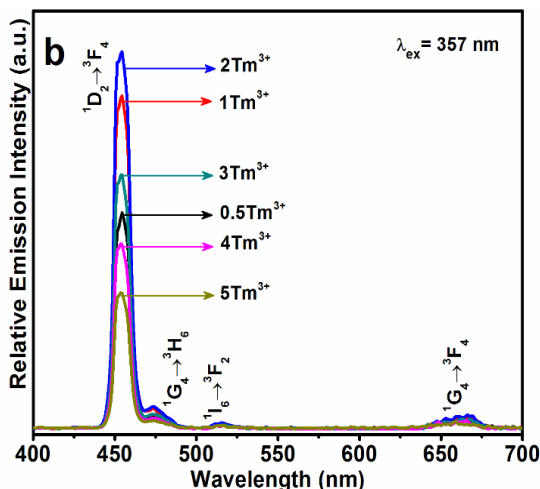


Fig.4. PL spectra of the SGSO: Tm^{3+} phosphors as a function of Tm^{3+} ion concentration.

Table.1: The calculated CIE coordinates (from PL spectra) of the SGSO: Tm^{3+} phosphors.

Phosphor	CIE coordinates
SGSO:0.5 Tm^{3+}	(0.1546, 0.0424)
SGSO:1 Tm^{3+}	(0.1514, 0.0357)
SGSO:2 Tm^{3+}	(0.1514, 0.0364)

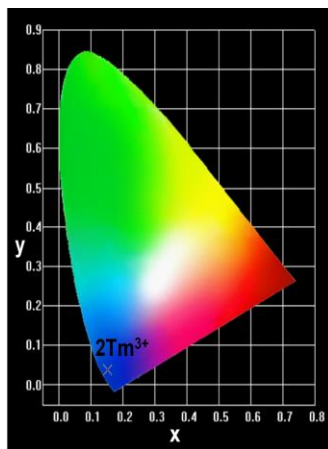


Fig.5. Color space representation of the PL spectrum of SGSO:2 Tm^{3+} phosphor produced CIE Chromaticity coordinates.

4. CONCLUSIONS

The SGSO:Tm³⁺ phosphors were successfully synthesized by a citrate sol-gel method. The X-ray diffraction pattern confirmed the hexagonal crystal form of oxyapatite structure with the space group of P6₃/m. The HR FE-SEM image showed the typical rod-like morphology with less aggregation. The PLE spectra exhibited an intense characteristic excitation peak at 357 nm in the lower energy region due to the 4f¹² intra-configurational ³H₆ → ¹D₂ transition of Tm³⁺ ions. The PL spectra of SGSO:Tm³⁺ phosphors showed the intense blue emission at 454 nm with the corresponding electronic ¹D₂ → ³F₄ transition. Thus, from the interesting CIE chromaticity coordinates of the PL spectra, the oxyapatite structured SGSO:Tm³⁺ phosphor is expected to be a promising material for potential applications in the development of efficient WLEDs and FED systems.

REFERENCES

- [1] E. Pavitra, G. Seeta Rama Raju, W. Park and J. S. Yu, *Title New J. Chem.*, 2014, **38**, 163-169.
- [2] V. C. Anitha, B. Arghya Narayan, J. Sang Woo and M. Bong Ki, *Nanotechnol.*, 2015, **26**, 355705.
- [3] D. Geng, G. Li, M. Shang, C. Peng, Y. Zhang, Z. Cheng and J. Lin, *Dalton Trans.*, 2012, **41**, 3078-3086.
- [4] G. Li and J. Lin, *Chem. Soc. Rev.*, 2014, **43**, 7099-7131.
- [5] X. Li, Y. Zhang, D. Geng, J. Lian, G. Zhang, Z. Hou and J. Lin, *J. Mater. Chem. C*, 2014, **2**, 9924-9933.
- [6] G. Seeta Rama Raju, E. Pavitra and J. S. Yu, *Dalton Trans.*, 2014, **43**, 9766-9776.
- [7] G. Seeta Rama Raju, J. Y. Park, H. C. Jung, E. Pavitra, B. K. Moon, J. H. Jeong, J. S. Yu, J. H. Kim and H. Choi, *J. Alloy. Compd.*, 2011, **509**, 7537-7542.
- [8] Y. Li, Y. H. Chang, Y.F. Lin, Y.J. Lin and Y. S. Chang, *Appl. Phys. Lett.*, 2006, **89**, 081110.
- [9] J. Hao, J. Gao and M. Cocivera, *Appl. Phys. Lett.*, 2003, **82**, 2224.
- [10] O. A. Lopez, J. McKittrick and L. E. Shea, *J. Lumin.*, 1997, **71**, 1.
- [11] Y. Nakanishi, H. Wada, H. Kominami, M. Kottaisamy, T. Aoki and Y. Hatanaka, *J. Electrochem. Soc.*, 1999, **146**, 4320.
- [12] X. M. Liu and J. Lin, *Appl. Phys. Lett.*, 2007, **90**, 184108.
- [13] R. P. Rao, *J. Lumin.*, 2005, **113**, 271.
- [14] A. L. Patterson, *Physical Review*, 1939, **56**, 978-982.
- [15] U. Holzwarth and N. Gibson, *Nat. Nano.*, 2011, **6**, 534-534.
- [16] N. Dhananjaya, H. Nagabhushana, B. Nagabhushana, B. Rudraswamy, C. Shivakumara and R. Chakradhar, *Bull. Mater. Sci.*, 2012, **35**, 519-527.
- [17] W. T. Carnall, P. R. Fields and K. Rajnak, *J. Chem. Phys.*, 1968, **49**, 4424-4442.